ENGINEERING OF ACIDIC O/W EMULSIONS WITH PECTIN

K. Alba[a], L.M.C. Sagis[b], V. Kontogiorgos[a*]

[a]Department of Biological Sciences, University of Huddersfield, HD1 3DH, UK

[b]Physics and Physical Chemistry of Food, Department AFSG, Wageningen University, Bornse Weilanden 9, 6708WG Wageningen, The Netherlands

*Corresponding author
Tel.: +44 1484 472488
e-mail: v.kontogiorgos@hud.ac.uk

Abstract

Pectins with distinct molecular design were isolated by aqueous extraction at pH 2.0 or 6.0 and were examined in terms of their formation and stabilisation capacity of model n-alkane–in–water emulsions at acidic pH (pH 2.0). The properties and stability of the resulting emulsions were examined by means of droplet size distribution analysis, Lifshitz-Slyozov-Wagner modelling, bulk rheology, interfacial composition analysis, large-amplitude oscillatory surface dilatational rheology, electrokinetic analysis and fluorescence microscopy. Both pectin preparations were able to emulsify alkanes in water but exhibited distinct ageing characteristics. Emulsions prepared using pectin isolated at pH 6.0 were remarkably stable with respect to droplet growth after thirty days of ageing, while those prepared with pectin isolated at pH 2.0 destabilised rapidly. Examination of chemical composition of interfacial layers indicated multi-layered adsorption of pectins at the oil-water interface. The higher long-term stability of emulsions prepared with pectin isolated at high pH is attributed to mechanically stronger interfaces, the highly branched nature and the low hydrodynamic volume of the chains that result in effective steric stabilisation whereas acetyl and methyl contents do not contribute to the long-term stability. The present work shows that it is possible by tailoring the fine structure of pectin to engineer emulsions that operate in acidic environments.

Keywords: pectin, emulsions, Ostwald ripening, Lissajous plots, fluorescence

1. Introduction

Emulsions are increasingly being utilized for encapsulating and delivering bioactives at targeted locations in the gastrointestinal tract [1]. A wide variety of lipophilic bioactives, including vitamins (D, E), carotenoids, flavonoids, phytosrerols, polyunsaturated lipids or flavours have been encapsulated in colloidal systems [2-6]. Emulsions as delivery vehicles allow sustained release and protection from degradation during storage of lipophilic bioactive components that are incorporated into the hydrophobic core of the lipid droplets. Furthermore, protection of the bioactive from environmental conditions (e.g., gastric fluids) when it is loaded in the internal phase of the emulsions is another advantage that may result in more efficient delivery.

Emulsions are most commonly formed using proteins or low molecular weight surfactants. The problem with such molecules when used as emulsifiers is that they have limited resistance to the gastric environment (e.g., proteases or low pH). These factors, among others, alter the surface composition and change the properties of the colloidal system [7, 8]. It is important, therefore, to control the physical stability within the stomach as a means to control the rate of release at the desired location (e.g., intestines or colon). Surface behaviour of emulsions can be tailored using surface-active polysaccharides with contrasting physical properties. Pectins from okra and sugar beet have unusual fine structures compared with other common pectin sources (e.g., citrus or apple), as they are highly acetylated and highly branched with variable amounts arabinan side chains and ferulic acid residues that ultimately control their functional properties [9-11]. Using pectin to engineer the oil-water interface could be favourable, as it is resistant to enzymatic digestion in the upper gastrointestinal tract (e.g., mouth and stomach),

nonetheless, is digested in the colon by pectinases. This functional characteristic makes pectin a suitable candidate to protect acid sensitive bioactives during gastric transit [12] or as a colon drug-delivery vehicle [13]. Other polysaccharide-based systems have been also tested as delivery methods due to biocompatibility and high potential to be modified and achieve the required functionality [14, 15].

In our previous investigations, we have tuned the extraction protocols of pectin from okra pods and obtained polysaccharides with tailored structure (e.g., molecular weight, branching, methoxyl and acetyl content, etc.) [16]. In the present work, we build on our previous experimental findings with the aim to understand the behaviour of pectin at the oil-water interfaces in highly acidic environments. We have, thus, engineered and characterised pectin-stabilized oil-in-water emulsions at low pH values (pH 2.0), as a first step to understand the underlying fundamental mechanisms of emulsion coarsening at pH values in the vicinity of gastric pH.

2. Materials and methods

2.1 Materials

Pectins were isolated from okra pods [16], labeled as OP2 and OP6 and their major physicochemical characteristics are shown in Table S1. Sodium azide, citric acid monohydrate, sodium citrate dihydrate, phenol, n-hexadecane, n-dodecane, formaldehyde (37-40%), phosphate buffer saline (PBS) (all analytical grade reagents) were obtained from Sigma-Aldrich (St Louis, MO). Anti-homogalacturonan antibody LM19 and LM4 (non-pectin specific antibody) were supplied by PlantProbes (Leeds, UK). De-ionized water was used throughout the experiments.

2.2 Preparation of emulsions

Preliminary experiments on the optimum concentration of pectin towards emulsion stability showed that fine emulsions are produced at pectin concentration of 1.5% w/v with dispersed phase volume fraction of $\varphi = 0.1$ (n-dodecane or n-hexadecane) and under acidic conditions (pH 2.0). The aqueous phases of the emulsions were prepared by means of dissolving pectin at 1.67% w/v concentration in citric buffer (10 mM, pH 2.0) at room temperature. Emulsions were fabricated at room temperature in two stages: a) pre-emulsions were obtained with a high-speed (IKA T18 basic, Ultra-Turrax, Germany) homogenizer for 2 min and, b) the coarse emulsions were further emulsified using an ultrasound device (Hielscher Ultrasonics, Model UP 100H) equipped with 7 mm diameter MS7 tip immersed (two-thirds) in the coarse emulsion and operating at 30 kHz. Ultrasonic treatment of the emulsions was performed for 40 s with pulsed ultrasound (30% per second) at 100% amplitude (corresponding to ultrasonic waves of 125 μm). The sonication conditions were chosen in accordance to the preliminary data that showed the absence of "over-processing".

2.3 Determination of droplet size distribution

Droplet size distribution was measured immediately after the emulsion preparation and after 1 h followed by measurements at 1, 10 and 30 days of storage at room temperature using a Malvern Mastersizer 2000 **(**Malvern Instruments Ltd, Worcestershire, UK**)** laser diffraction particle size analyzer equipped with the small volume sample dispersion unit Hydro 2000SM (Malvern Ltd, UK). Refractive indices of n-dodecane, n-hexadecane and dispersion medium (citric buffer, 10 mM, pH 2.0) were set to 1.421, 1.434 and 1.333, respectively. Consequently, droplet size was described

using the surface-weighted mean diameter ($d_{3,2}$), volume-weighted mean diameter ($d_{4,3}$) and span.

The physical properties of n-alkanes required for the calculations of theoretical (ω_{th}) Ostwald ripening rates in the emulsions were taken from literature [17-19]. Solubility ($c_{r\to\infty}$) was 2.3×10^{-5} and 9.3×10^{-8} (mol m^{-3}), diffusion coefficient (D) was 5.4 and 4.6 ($10^{-10} \times m^2\ s^{-1}$), molar volume ($V_m$) was 2.27 and 2.92 ($10^{-4} \times m^3$ mol) and molecular weight (M_w) was 0.170 and 0.226 (kg mol^{-1}) for n-dodecane and n-hexadecane, respectively. Interfacial tensions (γ) were 25.5 or 27.0 mN m^{-1} for n-hexadecane-water interfaces stabilized by 0.1% w/v OP6 or OP2, and 34.4 or 30.9 mN m^{-1} for n-dodecane-water interfaces stabilized by 0.1% w/v OP6 or OP2, respectively. Interfacial tension measurements were performed as described in section 2.5.

2.4 Interfacial composition analysis

Interfacial composition analysis was performed by determining protein, pectin and acetyl contents at the of oil-water interface. Emulsions were ultracentrifuged at 60000×g for 1 h (Optima L-100K ultracentrifuge, rotor 50.2 Ti, Beckman Coulter, USA) until equilibrium phase separation conditions were achieved and serum was collected using a syringe. The interfacial composition was evaluated as the protein, pectin or acetyl concentration difference between the pectin solutions (i.e., aqueous phase before emulsification) and serum solutions. Protein was measured with Bradford analysis using Quick Start™Bradford Protein Assay kit. The quantification of adsorbed pectin was expressed as total carbohydrates in pectin solution and serum phase using the phenol-sulphuric method [20]. The acetyl content was determined with the hydroxamic acid method in the pectin solution and serum phases [21]. Interfacial protein and pectin

concentrations (Γ, mg m^{-2}) were calculated as protein or pectin concentration difference between the biopolymer solution and serum phase divided by the specific surface area (SSA) of the oil droplets:

$$\Gamma = \frac{\text{mg of adsorbed protein or pectin}}{\text{SSA} \times \text{mL of alkane in emulsion}} \quad (1)$$

where specific surface area (SSA), m^2 mL^{-1} was obtained by the result analysis report of the instrument.

2.5 Interfacial rheology

The interfacial tension of the n-hexadecane- or n-dodecane- water interfaces stabilized by 0.1% w/v OP2 and OP6 was measured using a profile analysis tensiometer (PAT-1D, SINTERFACE Technologies, Berlin, Germany) at 20 °C. The n-alkane-water interfaces were equilibrated for 2 h and subjected to large-amplitude oscillatory dilatational deformations. The amplitude sweeps were performed stepwise from 2-50 % strain at a frequency 0.1 Hz. Lissajous plots were constructed by plotting the surface pressure $\pi = \gamma - \gamma_o$, where γ_o was interfacial tension before the oscillation, versus deformation $(A - A_o)/A_o$, where $A_o = 20$ mm^2 was the area at zero deformation.

2.6 Pectin immunolocalization at the o/w interface

Anti-homogalacturonan antibody LM19 [22] (PlantProbes, Leeds, United Kingdom) was used to localize pectin at the alkane-water interface and LM4 (non-pectin specific antibody) was used as a negative control.

Pectin aqueous phases with OP2 (1.67% w/v) were prepared in 10 mM PBS, pH 7.4. A drop of OP2 solution was placed on a microscopy slide and dried using Bunsen burner. Dried sample was fixed using 10% formalin solution buffered in 10 mM PBS.

Following the washing step, samples were blocked with 5% BSA in 10 mM PBS. The immunolabeling of pectic epitopes started with incubation of the samples with the primary antibody (LM19 was used as 5-fold dilution of a hybridoma supernatant) overnight at 4 °C followed by a washing step in PBS (three times for 5 min). LM19 was visualized using secondary labelling with anti-rat IgG coupled to fluorescein isothiocyanate (FITC) (Sigma-Aldrich, St. Louis, USA). The secondary antibody was diluted 1:5 in PBS and incubation was performed for 2 h at room temperature.

In order to use the probes for in situ immunolocalisation of pectin at the alkane-water interface, OP2-stabilized emulsions (1.5% w/v) were prepared using high-speed homogenizer (IKA T18 basic, Ultra-Turrax, Germany) for 2 min. Monoclonal antibody LM19 (100 μL, diluted 1:5) was added to 0.5 mL of coarse emulsion and left overnight at 4 °C. Subsequently, the secondary antibody IgG-FITC (100 μL, diluted 1:5) was added and emulsions were incubated for 2 h at room temperature. Emulsions were then centrifuged at 14100×g for 25 min (MiniSpin Plus, Eppendorf, Hamburg, Germany) in order to separate the droplets from the continuous phase. Immunostained emulsion droplets (diluted 1:10) and OP2 solutions were visualized using an Olympus IX70 microscope (Olympus, Optical Co. Ltd, Tokyo, Japan) equipped with epifluorescence illumination and using 10x and 40x oil immersion objectives. FITC was excited at 490 nm and emitted signal was collected between 528 and 538 nm. Image acquisition and analysis were performed with SoftWoRx software (Applied precision Inc.). The measurements were performed in duplicates in three different emulsion preparations yielding a total of six replicates for each sample.

3. Results and discussion

3.1 Emulsification capacity of pectin and ageing of emulsions

n-Hexadecane-in-water emulsions were stabilized by either pectin isolated at pH 2.0 (OP2) or pectin isolated at pH 6.0 (OP6). The change in droplet size distribution curves and the average droplet sizes were monitored for a period of 30 days (Table 1, Figures 1, 2). Both samples demonstrated good emulsification capacity producing emulsions with $d_{3,2}$ in the range of 1.7 – 3.0 μm (Table 1). Emulsions fabricated with OP6 demonstrated bimodal, broader droplet size distributions and were composed of droplets of larger diameters than those fabricated with OP2 pectin (Figures 1, 2, Table 1). These observations are in a good agreement with interfacial tension measurements where a faster decrease of interfacial tension was observed in for OP2 (Figure S2).

Zero-shear viscosity of OP6 solutions at the concentrations used in the continuous phases was greater compared to OP2 counterparts (Figure S1). This impedes the induction of cavitation phenomena [23] during fabrication of OP6-stabilized emulsions resulting in bimodal droplet size distributions (Figure 1). Instability in bimodal colloidal dispersions is usually controlled by the higher modes resulting in the predominance of coalescence as the major destabilisation mechanism [24]. However, OP6-stabilized emulsions did not exhibit any appreciable development of coalescence–induced second peak during ageing as indicated by the droplet sizes and span of droplet distributions (Figure 1, Table 1). These observations are in a good agreement with the rheological measurements (Figure S1a) that do not show any appreciable changes in viscosity curves indicating limited microstructural reorganisation (e.g., flocculation) during the period of thirty days. Coalescence typically increase the polydispersity and accelerate the rate of

coarsening [25], as it is easily observed in OP2-stabilized emulsions. Emulsions prepared with OP2 destabilised rapidly and demonstrated a marked increase in average droplet size, with $d_{4,3}$ rising from 2.4 to 10.0 μm within 1 h of storage (Figure 2). Considerable destabilisation occured after one day of storage and continued unabated for thirty days (Figure 2, Table 1). Additionally, the rheological measurements of OP2-stabilized emulsions (Figure S1b) revealed a considerable increase of zero-shear viscosity during ageing that is attributed to depletion flocculation caused by pectin desorption from the interface during coarsening.

Overall, OP6-stabilized emulsions exhibited remarkable stability during ageing as opposed to the OP2-stabilized counterparts. Contrasting stabilities of this magnitude pronounce that differences in the fine stucture and conformation at low pH of the isolated polyelecrolytes play a predominant role in the emulsification capacity. In the following sections we delve further into the molecular mechanisms of instability in an effort to shed light on the structure versus function relation of these intricate biopolymers.

3.2 Examination of destabilisation mechanisms

In this part of the investigation, we start by employing the Lifshitz–Slyozov–Wagner (LSW) theoretical framework [26] to assess the potential role of Ostwald ripening in the evolution of droplet size. In a typical Ostwald ripening scenario, at asymptotically long times, the change in number droplet diameter cubed is a linear function of time and is given by:

$$d_t^3 - d_{t=0}^3 = \left(\frac{64\gamma D c_{r\to\infty} V_m^2 t}{9RT} \right) = \omega t \qquad (2)$$

where t is the time, d_t is the surface mean diameter ($d_{3,2}$) after time t, $d_{t=0}$ is the initial surface mean diameter, γ is the interfacial tension of the oil-water interface, D is the diffusion coefficient of the oil through the aqueous (continuous) phase, $c_{r\to\infty}$ is the solubility of the oil in the aqueous phase, V_m is the molar volume of the oil, R is the gas constant, T is the absolute temperature and ω is the Ostwald ripening rate. Brownian motion-induced coalescence also results in a linear correlation of droplet growth rate as a function of time [27] but is not expected to influence the destabilisation of the dispersions of the present study due to the predominance of gravity as evidenced by the droplet sizes (1.7–3.0 μm). The examination of coarsening mechanisms was performed under conditions where one type of instability dominates over the other in order to monitor its progress more accurately. Preliminary data have shown that an increase of pectin concentration beyond 1.5% w/v did not result in further reduction of droplet diameter, indicating saturation of the n-alkane-water interface. A sufficient surface coverage of droplets with emulsifier ensures that coalescence (i.e., collision-induced coalescence) does not dominate the destabilisation kinetics and enables monitoring of Ostwald ripening with minimum interference from coalescence at the early stages of the coarsening process. The change in $(d_{3,2})^3$ vs. time of n-hexadecane-in-water emulsions was monitored for 1 h with 5 min intervals and demonstrated a linear increase of $(d_{3,2})^3$ with time (Figure 3). We plotted the $d_{3,2}$ radius rather than the number mean radius ($d_{1,0}$) as is dictated by the theory, since the surface mean diameter can be more accurately determined by laser light scattering [28].

Droplet size did not develop appreciably for OP6-stabilized emulsions throughout the observation period making it difficult to ascribe the changes to Ostwald ripening. In

contrast, OP2-stabilised emulsions exhibited considerably steeper slope than their OP6 counterparts indicating higher experimental rate of droplet growth (Table 2). The linearity of $(d_{3,2})^3$ vs. time plots cannot be solely utilized in the assessment of instability mechanisms in such complex colloidal systems and the possible origins of emulsion coarsening can be further established with changes in the alkane chain length [17, 29, 30]. The solubility of alkanes in water vary considerably with molecular weight thus influencing Ostwald ripening rates (Equation 2). In order to address the above, OP2 and OP6 stabilized emulsions were fabricated with n-dodecane and their $d_{3,2}$, $d_{4,3}$, droplet size distributions and experimental coarsening rates were compared with those prepared with n-hexadecane (insets of Figures 1, 2, Table 1, Figure 3 and Table 2). Analysis of $(d_{3,2})^3$ vs. time plots and calculation of experimental growth rates (ω_{exp}) for OP6-stabilized emulsions show modest changes in emulsion coarsening rate within 1 h (Figure 3, Table 2). Conversely, emulsions fabricated with OP2 demonstrate appreciable increase in coarsening kinetics on replacing n-hexadecane with n-dodecane (Figure 2 (inset), Figure 3 and Table 2) suggesting the occurrence of Ostwald ripening in the first hour of ageing for OP2 stabilized emulsions. Moreover, theoretical modeling of droplet growth rate has shown that the change in ripening rates is several orders of magnitude higher for n-dodecane than n-hexadecane, something that was not reflected by the experimental growth rates (ω_{exp}) (Table 2).

Taking everything into account, it has been shown that pectin-stabilized emulsions evolve under complex destabilisation mechanisms that could be characterized by Ostwald ripening in conjunction with coalescence. Pectin fine structure controls the interplay between these two mechanisms as greater degree of branching of OP6 (HG/RG

ratio, Table S1) hinders droplet growth and provides long-term stability. Typically, high molecular weight polysaccharides are weakly adsorbing biopolymers and undergo intra- and intermolecular rearrangements at the interface during storage. As droplet size develops, conformational rearrangement at the interface results in thinning of the interfacial film and formation of thermally activated "holes" that extend across the interfacial membranes. These microstructural modifications eventually lead to the emergence of coalescence. Other schools of thought interpret the interplay between Ostwald ripening and coalescence using the molecular permeation theory [31] or focusing on the process of molecular exchange of oil molecules upon droplet collision [32]. Such destabilisation mechanisms are frequently reported for biopolymer- [30, 33] or synthetic polymer- [25] stabilised alkane emulsions where the coarsening mechanism is ascribed to Ostwald ripening-induced coalescence.

It starts emerging that the structural features of these biopolymers control the remarkable variations in the temporal evolution of coarsening. Examination of the interfacial composition will further elucidate what are the key structural features responsible for these striking differences in their stability.

3.3 Interfacial composition analysis

The interfacial activity of pectin and ability to stabilize emulsions are attributed to the molecular weight, methoxyl and acetyl content, degree of branching, presence of ferulic groups and proteinaceous components in the biopolymer backbone [34-36]. Table 3 shows the interfacial composition of OP2 and OP6-stabilized n-hexadecane-in-water emulsions revealing that comparable amount of acetyl was adsorbed at the interface in both systems. These results are also in a good agreement with the chemical composition

data that report marginal differences in the concentration of acetyl groups (Table S1). Since both biopolymers have similar amounts of acetyl adsorbed at the interface as well as absence of ferulic acids these two parameters do not seem to be responsible for the differences in emulsification capacity and emulsion stability.

Protein surface coverage of OP6-stabilized emulsions was 1.6 mg m^{-2} a value five-times higher than that of the OP2-stabilized emulsions (0.3 mg m^{-2}). Protein content is comparable in both samples (Table S1) and differences in protein adsorption suggest that accessibility of the protein to the interface and its amino acid composition influence the emulsification properties of the present samples. Previous studies also reported that the pectin fraction adsorbed at the interface was significantly enriched in protein and played a key role in emulsion stabilizing capacity [36-38]. However, protein surface coverage alone cannot explain the striking differences in the stability of emulsions, as it will be discussed below. The surface coverage with pectin in OP6-stabilized emulsions was 9.4 mg m^{-2} whereas OP2 systems had considerably lower pectin interfacial load (3.3 mg m^{-2}). Surface coverage with pectin in OP6-stabilized emulsions was higher than previously reported for sugar beet pectin [36, 38] (~ 7.5 mg m^{-2}) at the same polymer concentration and comparable with depolymerized citrus pectin (~ 9.8 mg m^{-2}) [38].

Comparison of the amount of adsorbed protein and pectin indicates that the interfaces are dominated by the presence of pectin. This is further supported by the negative ζ-potential values at pH 2.0 for both emulsions denoting that the n-hexadecane-in-water interface has similar electrical properties to that of the continuous phase (Figure S4). Low ζ-potential values for fresh OP2 and OP6 stabilized emulsions also indicate that electrostatic repulsions do not have significant effect on the overall stability of the

dispersions. As a consequence, the proteinaceous components, as an integral part of the samples, anchor pectin at the n-alkane-water interface, the polysaccharides protrude out into the continuous phase and provide an effective steric barrier [36, 37]. Multilayer adsorption has been previously reported for the naturally occurring polysaccharide–protein complexes, such as arabic gum and sugar beet pectin [39]. Furthermore, the higher pectin interfacial load in OP6-stabilized emulsions and higher degree of branching of OP6 (Table S1) denote the presence of more effective steric barrier than in OP2-stabilized emulsions. These results are in a good agreement with ageing data of OP6-stabilized emulsions that showed negligible droplet growth with time in comparison to the OP2 counterparts (Figures 1, 2; Table 1).

3.4 Interfacial rheology at the n-alkane-water interface

The analysis of interfacial composition suggests that a thin biopolymer film is formed in emulsions stabilized with OP2 that could lead to mechanically weak interface. On the other hand, emulsions stabilized with OP6 demonstrated higher interfacial loads resulting in formation of thicker interfacial layers that hinder droplet growth. Therefore, n-alkane-water interfaces stabilized by OP2 or OP6 were subjected to large-amplitude oscillatory dilatational deformations in order to evaluate the mechanical rigidity of the adsorbed layers. Lissajous plots of surface pressure versus deformation were constructed in order to analyse the nonlinear dilatational behaviour (Figure 4). The Lissajous plots for both pectin stabilized n-alkane-water interfaces were asymmetric indicating that the responses of the interfaces in extension were different than in compression. At the limits of the experimental amplitudes, the surface pressure in compression was almost twice as high (~15.0×10^{-3} N m^{-1}) as the surface pressure in extension (~8.0×10^{-3} N m^{-1}) with

differences being more pronounced with n-dodecane. The shape of the curves indicated that upon compression the surface displays strain hardening behaviour, whereas in extension the interface displays strain softening behaviour [40]. The softening is more pronounced in the interfaces stabilized by OP2, than in those stabilized by OP6. This particular shape of the Lissajous plots indicates that the pectin molecules are not forming a highly interconnected and elastic network at the alkane-water interface, as is often observed in pure protein stabilized interfaces. The latter typically display strain-hardening behaviour both in compression and extension. This again shows that the protein matter in the system does not play a dominant role in the stability of the emulsions. The shape of our plots is more typical for weakly aggregated two-dimensional (2d) gels or 2d soft glasses. Upon compression the adsorbed protein-pectin complexes become jammed, which leads to the observed strain hardening. Upon extension the surface fraction of pectins decreases and the structure loses connectivity, resulting in the observed softening. Similar behaviour has been previously observed for protein fibrils and was also attributed to the structural rearrangements of biopolymer macrostructures at the interface due to the applied deformation [41, 42]. The dependence of Lissajous plot shape on the deformation amplitude was further examined for n-hexadecane-water interfaces stabilized by OP2 and OP6 (Figure S3). These observations indicate that interfaces stabilized by OP6 were more resistant to deformation in comparison to those stabilized with OP2. The variations in viscoelastic properties of the interfaces are attributed to the structural and conformational differences of the samples. OP6 is composed of polymer chains with higher degree of branching and occupy lower hydrodynamic volume ($[\eta]_{OP6} < [\eta]_{OP2}$) than the OP2 counterparts indicating the formation of more compact structures (Table S1). These

results combined with the interfacial composition analysis (Table 3) give strong evidence that thicker interfaces are formed with OP6, with higher values for their dilatational moduli, which impede Ostwald ripening and coalescence resulting in prevention of droplet coarsening.

3.5 Pectin immunolocalisation at the alkane-water interface.

In the last part of the investigation we provide tangible evidence of the presence of pectin at the droplet interfaces by fluorescence immunolocalisation. Figures 5 and Figure S5 show maximum intensity z-projected images of the morphology of OP2 solutions and emulsions. Figures S5a-c correspond to the micrographs of controls that included OP2 solution, OP2 solution with anti-rat IgG coupled with FITC and OP2 solution with a negative control, respectively. A weak signal was spread evenly over the polymer sample and can be attributed to the intrinsic fluorescence emission of pectin. It has been previously reported that pectin demonstrates auto-fluorescence at around 530-550 nm [43]. Figure S5d shows that LM19 binds to the HG domains of OP2 as evidenced by the presence of small entities (arrows). The binding specificity of LM19 antibodies in pectin solutions was established with indirect immunostaining, a methodology that is not achievable with the dispersed systems. Therefore, direct immunostaining was used to localize pectin at alkane- water interfaces (Figure 5a, b and Figure S5h). Pectin-stabilized emulsions do not show any fluorescence emission whereas those emulsions containing fluorescent dye exhibit a weak signal due to possible aggregation of IgG-FITC (Figure S5e-g). Figure 5 a, b provides evidence that pectin adsorbs at the droplet interface providing complete coverage of the droplet interface with pectin revealing the clear

predominance of pectin over protein at the interface of the emulsions. It should be stressed that images were z-projected and therefore, they demonstrate the network (in case of solutions) and droplet (in emulsion) in three dimensions from top to bottom of the image plane (Figures 5, Figure S5).

4. Conclusions

The influence of molecular architecture of pectin on emulsifying capacity has been investigated by means of an array of complimentary physical and chemical analyses. It has been shown that pectin exhibits interfacial activity and stabilises emulsions by formation of elastic protein-polysaccharide bilayers that prevent droplet growth. Protein component, which is inevitably present, is not the predominant factor responsible for emulsion formation and stabilisation.

Remarkable long-term stability of emulsions was achieved only with pectin extracted at high pH values (pH 6) due to the highly branched nature and low hydrodynamic volume of its chains that contribute to effective steric stabilisation whereas acetyl and methyl contents do not contribute to the long-term stability. On the contrary emulsions stabilised with pectin extracted at low pH (pH 2) destabilise rapidly following a complex mechanism that has been identified as combination of Ostwald ripening at the initial stages followed by coalescence. The present work uncovered the link between the fundamental molecular properties of pectin with its interfacial functionality, as a first step to engineering bioresponsive emulsions that can operate at low pH environments.

Acknowledgements: The authors gratefully acknowledge the financial support provided by the GEN Foundation, and Prof. P. Knox (University of Leeds, UK) for the kind donation of pectin antibodies.

5. References

[1] S. Abbas, K. Hayat, E. Karangwa, M. Bashari, X. Zhang, An Overview of Ultrasound-Assisted Food-Grade Nanoemulsions, Food Eng. Rev. 5 (2013) 139-157.

[2] M. Guttoff, A.H. Saberi, D.J. McClements, Formation of vitamin D nanoemulsion-based delivery systems by spontaneous emulsification: Factors affecting particle size and stability, Food Chem. 171 (2015) 117-122.

[3] S. Mayer, J. Weiss, D.J. McClements, Vitamin E-enriched nanoemulsions formed by emulsion phase inversion: Factors influencing droplet size and stability, J. Colloid Interface Sci. 402 (2013) 122-130.

[4] D.J. McClements, Nanoemulsions versus microemulsions: terminology, differences, and similarities, Soft Matter, 8 (2012) 1719-1729.

[5] D.J. McClements, E.A. Decker, Y. Park, J. Weiss, Structural Design Principles for Delivery of Bioactive Components in Nutraceuticals and Functional Foods, Crit. Rev. Food Sci. Nutr. 49 (2009) 577-606.

[6] D.J. McClements, J. Rao, Food-Grade Nanoemulsions: Formulation, Fabrication, Properties, Performance, Biological Fate, and Potential Toxicity, Crit. Rev. Food Sci. Nutr. 51 (2011) 285-330.

[7] H. Singh, A. Ye, D. Horne, Structuring food emulsions in the gastrointestinal tract to modify lipid digestion, Prog. Lipid Res. 48 (2009) 92-100.

[8] I.J. Joye, D.J. McClements, Biopolymer-based nanoparticles and microparticles: Fabrication, characterization, and application, Curr. Opin. Colloid Interface Sci. 19 (2014) 417-427.

[9] N. Sengkhamparn, L.M.C. Sagis, R. de Vries, H.A. Schols, T. Sajjaanantakul, A.G.J. Voragen, Physicochemical properties of pectins from okra (Abelmoschus esculentus (L.) Moench), Food Hydrocolloids, 24 (2010) 35-41.

[10] V. Kontogiorgos, I. Margelou, N. Georgiadis, C. Ritzoulis, Rheological characterization of okra pectins, Food Hydrocolloids, 29 (2012) 356-362.

449 [11] K. Alba, C. Ritzoulis, N. Georgiadis, V. Kontogiorgos, Okra extracts as emulsifiers
450 for acidic emulsions, Food Res. Int. 54 (2013) 1730-1737.

451 [12] M.U. Ghori, K. Alba, A.M. Smith, B.R. Conway, V. Kontogiorgos, Okra extracts in
452 pharmaceutical and food applications, Food Hydrocolloids, 42 (2014) 342-347.

453 [13] C.-Y. Yu, H. Cao, X.-C. Zhang, F.-Z. Zhou, S.-X. Cheng, X.-Z. Zhang, Zhuo R. X.
454 Hybrid nanospheres and vesicles based on pectin as drug carriers, Langmuir, 25 (2009)
455 11720-11726.

456 [14] M. Fathi, A. Martin, D.J. McClements, Nanoencapsulation of food ingredients using
457 carbohydrate based delivery systems, Trends Food Sci. Technol. 39 (2014) 18-39.

458 [15] V. Kontogiorgos, A.M. Smith, G.A. Morris, The parallel lives of polysaccharides in
459 food and pharmaceutical formulations, Curr. Opin. Food Sci. 4 (2015) 13-18.

460 [16] K. Alba, A.P. Laws, V. Kontogiorgos, Isolation and characterisation of acetylated
461 LM-pectins extracted from okra pods, Food Hydrocoilloids, 43 (2015) 726-735.

462 [17] J. Weiss, N. Herrmann, D.J. McClements, Ostwald Ripening of Hydrocarbon
463 Emulsion Droplets in Surfactant Solutions, Langmuir, 15 (1999) 6652-6657.

464 [18] C.R. Wilke, P. Chang, Correlation of diffusion coefficients in dilute solutions,
465 AIChE J. 1 (1955) 264-270.

466 [19] R. Aveyard, D.A. Haydon, Thermodynamic properties of aliphatic
467 hydrocarbon/water interfaces, Trans. Faraday Soc. 61 (1965) 2255.

468 [20] M. Dubois, K.A. Gilles, J.K. Hamilton, P.A. Rebers, F. Smith, Colorimetric method
469 for determination of sugars and related substances, Anal. Chem. 28 (1956) 350-356.

470 [21] E.A. McComb, R.M. McCready, Determination of acetyl in pectin and in acetylated
471 carbohydrate polymers., Anal. Chem. 29 (1957) 819–921.

472 [22] Y. Verhertbruggen, S.E. Marcus, A. Haeger, J.J. Ordaz-Ortiz, J.P. Knox, An
473 extended set of monoclonal antibodies to pectic homogalacturonan, Carbohydr. Res. 344
474 (2009) 1858−1862.

475 [23] N.A. Camino, C.C. Sánchez, J.M. Rodríguez Patino, A.M.R. Pilosof,
476 Hydroxypropylmethylcellulose at the oil–water interface. Part I. Bulk behaviour and
477 dynamic adsorption as affected by pH, Food Hydrocolloids, 25 (2011) 1-11.

478 [24] D.J. McClements, Food Emulsions-principles, practice and techniques, CRC Press
479 LLC, New York, 1999.

480 [25] V. Schmitt, C. Cattelet, F. Leal-Calderon, Coarsening of Alkane-in-Water Emulsions
481 Stabilized by Nonionic Poly(oxyethylene) Surfactants: The Role of Molecular
482 Permeation and Coalescence, Langmuir, (2004) 46-52.

[26] I.M. Lifshitz, V.V. Slyozov, The kinetics of precipitation from supersaturated solid solutions, J. Phys. Chem. Solids. 19 (1961) 35-50.

[27] H. Wang, R.H. Davis, Droplet growth due to Brownian, gravitational, or thermocapillary motion and coalescence in dilute emulsions, J. Colloid Interface Sci. 159 (1993) 108-118.

[28] M.B.J. Meinders, W. Kloek, T. Van Vliet, Effect of surface elasticity on Ostwald ripening in emulsions, Langmuir, 17 (2001) 3923-3929.

[29] A.S. Kabalnov, E.D. Shchukin, Ostwald ripening theory: applications to fluorocarbon emulsion stability, Adv. Colloid Interface Sci. 38 (1992) 69-97.

[30] R. Chanamai, G. Horn, D.J. McClements, Influence of Oil Polarity on Droplet Growth in Oil-in-Water Emulsions Stabilized by a Weakly Adsorbing Biopolymer or a Nonionic Surfactant, J. Colloid Interface Sci., 247 (2002) 167-176.

[31] K. Pays, J. Giermanska-Kahn, B. Pouligny, J. Bibette, F. Leal-Calderon, Coalescence in surfactant-stabilized double emulsions, Langmuir, 17 (2001) 7758-7769.

[32] K. Roger, U. Olsson, R. Schweins, B. Cabane, Emulsion ripening through molecular exchange at droplet contacts, Angew. Chem. Int. Ed. Engl. (2015) 54, 1452-1455.

[33] E. Dickinson, C. Ritzoulis, Y. Yamamoto, H. Logan, Ostwald ripening of protein-stabilized emulsions: effect of transglutaminase crosslinking, Colloids Surf., B. (1999) 139–146.

[34] I.C.M. Dea, J.K. Madden, Acetylated pectic polysaccharides of sugar beet, Food Hydrocolloids, 1 (1986) 71-88.

[35] U.S. Schmidt, L. Koch, C. Rentschler, T. Kurz, H.U. Endreß, H.P. Schuchmann, Effect of Molecular Weight Reduction, Acetylation and Esterification on the Emulsification Properties of Citrus Pectin, Food Biophysics, (2014) 10, 217-227

[36] C.K. Siew, P.A. Williams, Role of protein and ferulic acid in the emulsification properties of sugar beet pectin, J. Agric. Food Chem. 56 (2008) 4164-4171.

[37] J. Leroux, V. Langendorff, G. Schick, V. Vaishnav, J. Mazoyer, Emulsion stabilizing properties of pectin, Food Hydrocolloids, 17 (2003) 455-462.

[38] M. Akhtar, E. Dickinson, J. Mazoyer, V. Langendorff, Emulsion stabilizing properties of depolymerized pectin, Food Hydrocolloids, 16 (2002) 249-256.

[39] M. Evans, I. Ratcliffe, P.A. Williams, Emulsion stabilisation using polysaccharide-protein complexes, Curr. Opin. Colloid Interface Sci. 18 (2013) 272-282.

[40] S.E.H.J. Van Kempen, H.A. Schols, E. Van Der Linden, L.M.C. Sagis, Non-linear surface dilatational rheology as a tool for understanding microstructures of air/water interfaces stabilized by oligofructose fatty acid esters, Soft Matter, 9 (2013) 9579-9592.

[41] S. Jordens, L. Isa, I. Usov, R. Mezzenga, Non-equilibrium nature of two-dimensional isotropic and nematic coexistence in amyloid fibrils at liquid interfaces, Nat. Commun. 4 (2013).

[42] L.M.C. Sagis, K.N.P. Humblet-Hua, S.E.H.J. Van Kempen, Nonlinear stress deformation behavior of interfaces stabilized by food-based ingredients, J. Phys.: Condens. Matter. 26 (2014) 464105.

[43] L.S. Liu, T. Jin, C.K. Liu, K. Hicks, A. Mohanty, R. Bhardwaj, M. Misra, A preliminary study on antimicrobial edible films from pectin and other food hydrocolloids by extrusion method, J. Nat. Fibers. 5 (2008) 366-382.

[44] Y. Enomoto, M. Tokuyama, K. Kawasaki, Finite volume fraction effects on Ostwald ripening, Acta Metall. 34 (1986) 2119-2128.

Tables

Table 1. Influence of pectin type and ageing on the average droplet diameters ($d_{3,2}$ and $d_{4,3}$) and span in n-dodecane and n-hexadecane emulsions formed with 1.5% (w/v) OP2 and OP6.

Sample	Time	$d_{3,2}$ (μm)		$d_{4,3}$ (μm)		Span	
		$C_{12}H_{26}$	$C_{16}H_{34}$	$C_{12}H_{26}$	$C_{16}H_{34}$	$C_{12}H_{26}$	$C_{16}H_{34}$
OP2	Fresh	1.8 ± 0.1	1.7 ± 0.1	2.6 ± 0.1	2.4 ± 0.1	2.0 ± 0.0	1.8 ± 0.0
	1 h	5.1 ± 0.2	4.1 ± 0.1	11.9 ± 0.4	10.0 ± 0.4	2.5 ± 0.0	2.7 ± 0.0
	1day	5.7 ± 0.1	4.6 ± 0.2	52.2 ± 1.4	34.5 ± 1.7	7.0 ± 0.2	7.5 ± 0.2
	10 days	7.0 ± 1.3	5.5 ± 1.1	122.5±38.2	107.9±21.2	11.0 ± 1.6	11.4 ± 2.6
	30 days	8.7 ± 1.3	6.0 ± 0.2	162.4±30.8	132.7±0.9	3.0 ± 0.3	3.6 ± 0.2
OP6	Fresh	2.8 ± 0.5	3.0 ± 0.3	7.6 ± 2.6	7.3 ± 1.9	2.9 ± 0.5	3.0 ± 0.1
	1 h	3.3 ± 0.8	3.1 ± 0.5	11.2 ± 2.6	7.4 ± 1.1	2.7 ± 0.1	2.5 ± 0.1
	1day	5.0 ± 0.1	3.2 ± 0.4	11.8 ± 0.9	7.7 ± 0.4	2.2 ± 0.2	2.4 ± 0.3
	10 days	9.1 ± 0.2	4.1 ± 4.1	19.2 ± 1.3	10.5 ± 2.1	2.2 ± 0.1	2.4 ± 0.3
	30 days	8.9 ± 0.2	4.5 ± 0.4	20.7 ± 0.9	11.4 ± 1.2	2.2 ± 0.1	2.4 ± 0.1

Table 2. Theoretical (ω_{th}) and experimental (ω_{exp}) rates of Ostawld ripening for various oil-in-water emulsions.

Sample	OP2		OP6	
n-alkane type	$C_{12}H_{26}$	$C_{16}H_{34}$	$C_{12}H_{26}$	$C_{16}H_{34}$
ω_{th} [a] ($m^3\ s^{-1}$) 10^{-26}	9.9	0.049	11.1	0.047
ω_{exp} [b] ($m^3\ s^{-1}$) 10^{-21}	26.0 (±4 10^{-3})	21.0 (±3 10^{-3})	2.6 (±6 10^{-3})	2.5 (±0.22 10^{-3})

[a] Theoretical rate (ω_{th}) of Ostwald ripening was calculated with Eq., 2 using the physical parameters mentioned in section 2.3 and corrected by a factor k_f = 1.75 that reflects the dependence of the coarsening rate on the dispersed phase volume fraction φ = 0.1.[44]

[b] Experimental rate calculated based from data shown in Figure 3

Table 3. Weight percentage and amount of adsorbed protein, pectin and acetyl at the oil-water interface of fresh w/v n-hexadecane emulsions stabilized with OP2 or OP6 at φ = 0.1, pH 2.0.

Sample	OP2	OP6
Adsorbed acetyl (%)	9.7 ± 0.4	9.1 ± 0.6
Adsorbed protein (mg m^{-2})	0.3 ± 0.1	1.6 ± 0.5
Adsorbed protein (%)	17.1 ± 6.0	49.5 ± 15.6
Adsorbed pectin (mg m^{-2})	3.3 ± 0.2	9.4 ± 0.2
Adsorbed pectin (%)	14.2 ± 1.1	16.3 ± 5.7

Figure captions

Figure 1. Droplet size distribution curve development of n-hexadecane-in-water emulsion stabilized with OP6 at 25 °C for thirty days of ageing. Inset shows droplet size distribution curves of n-dodecane-in-water emulsion stabilized with OP6 at 25 °C for thirty days of ageing.

Figure 2. Droplet size distribution curve development of n-hexadecane-in-water emulsion stabilized with OP2 at 25 °C for thirty days of ageing. Inset shows droplet size distribution curves of n-dodecane-in-water emulsion stabilized with OP2 at 25 °C for thirty days of ageing.

Figure 3. Dependence ($(d_{3,2})^3$ vs. time) of Ostwald ripening rates on n-hydrocarbon type in OP2 or OP6 stabilized emulsions at pH 2.0 (25 °C).

Figure 4. Lissajous plots for a) n-hexadecane-, and b) n-dodecane-water interfaces stabilized by OP2 and OP6. Droplet area 20 mm^2, strain amplitude 50%, frequency 0.1 Hz.

Figure 5. Fluorescent images of 1.5% w/v n-dodecane-in-water OP2-stabilized emulsions at pH 7.4 a) middle plane and b) z-projected images.

608 **Graphical abstract**

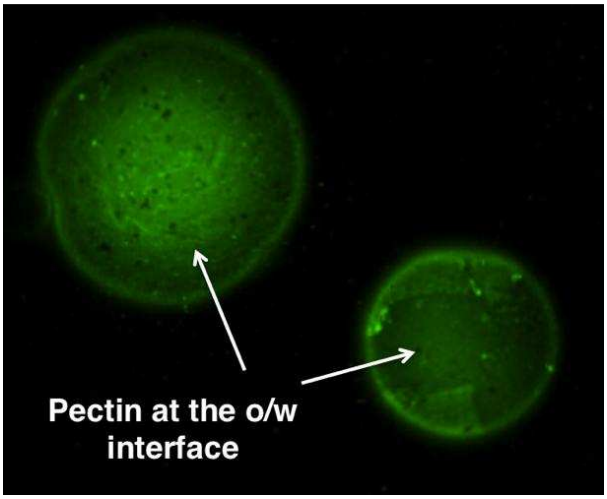

609

610

611

612

613

614

615

616

Figure-1

Figure 1

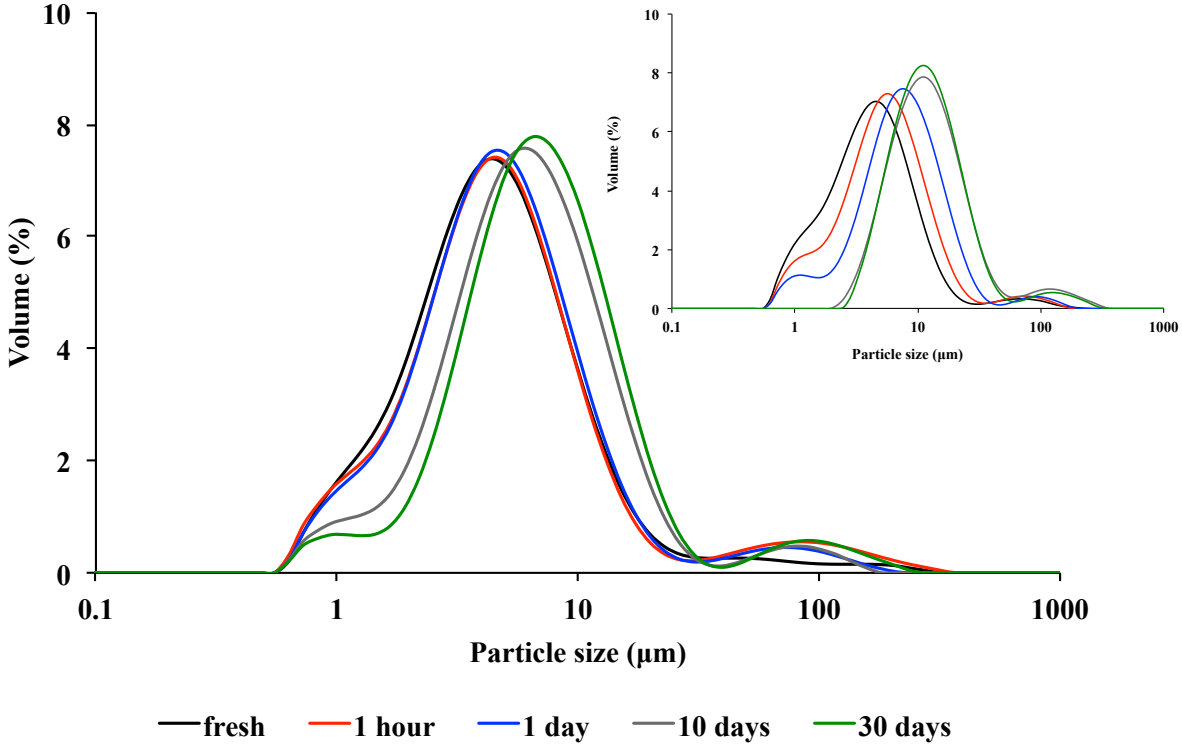

Figure 2.

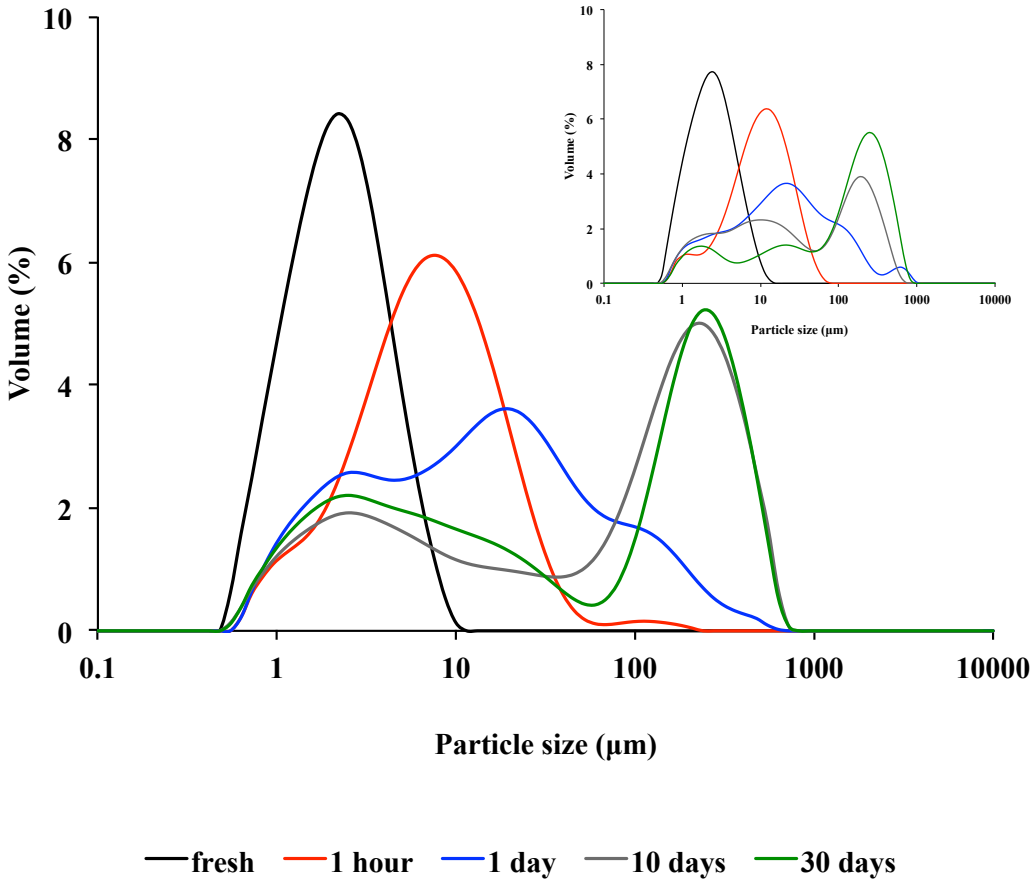
Volume (%)
Particle size (µm)
0.1
1
10
100
1000
10000
0
2
4
6
8
10
fresh
1 hour
1 day
10 days
30 days

Figure 3

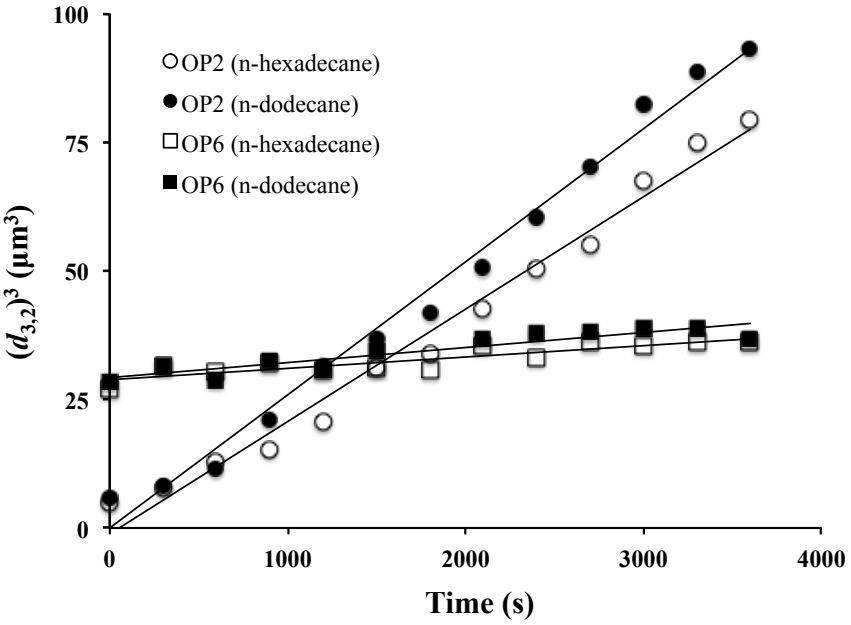
100
75
50
25
0
0
1000
2000
3000
4000
Time (s)
$(d_{3,2})^3$ (µm^3)
OP2 (n-hexadecane)
OP2 (n-dodecane)
OP6 (n-hexadecane)
OP6 (n-dodecane)

Figure-4

Figure 4

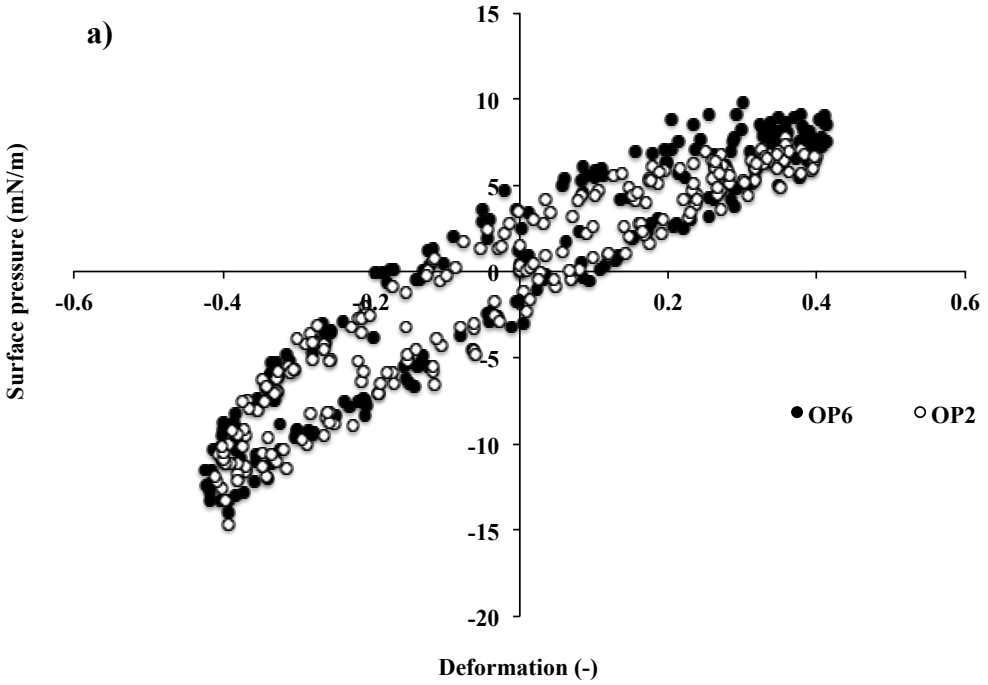

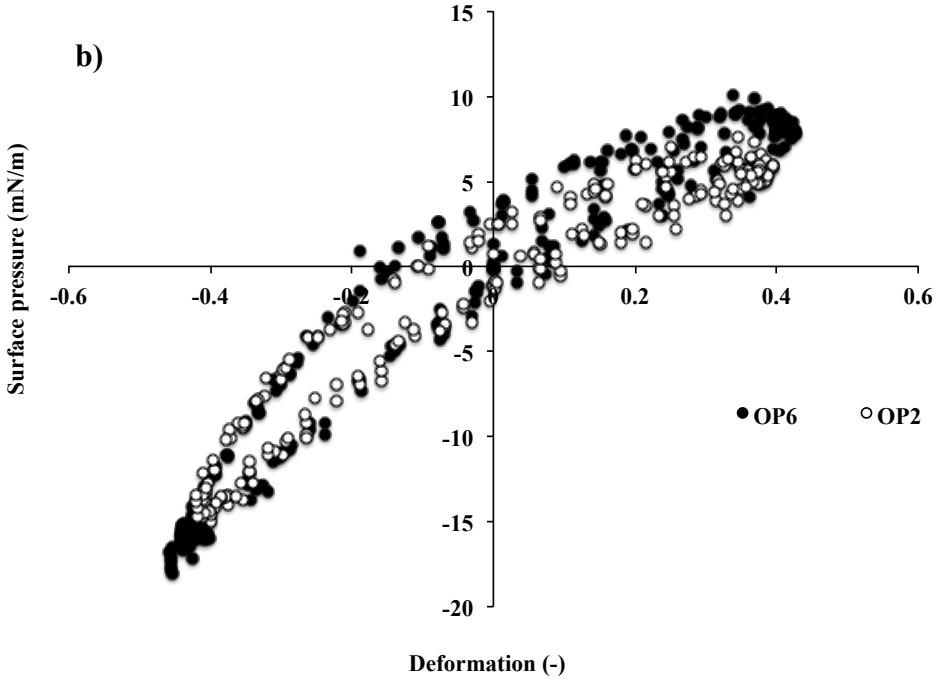

Figure-5

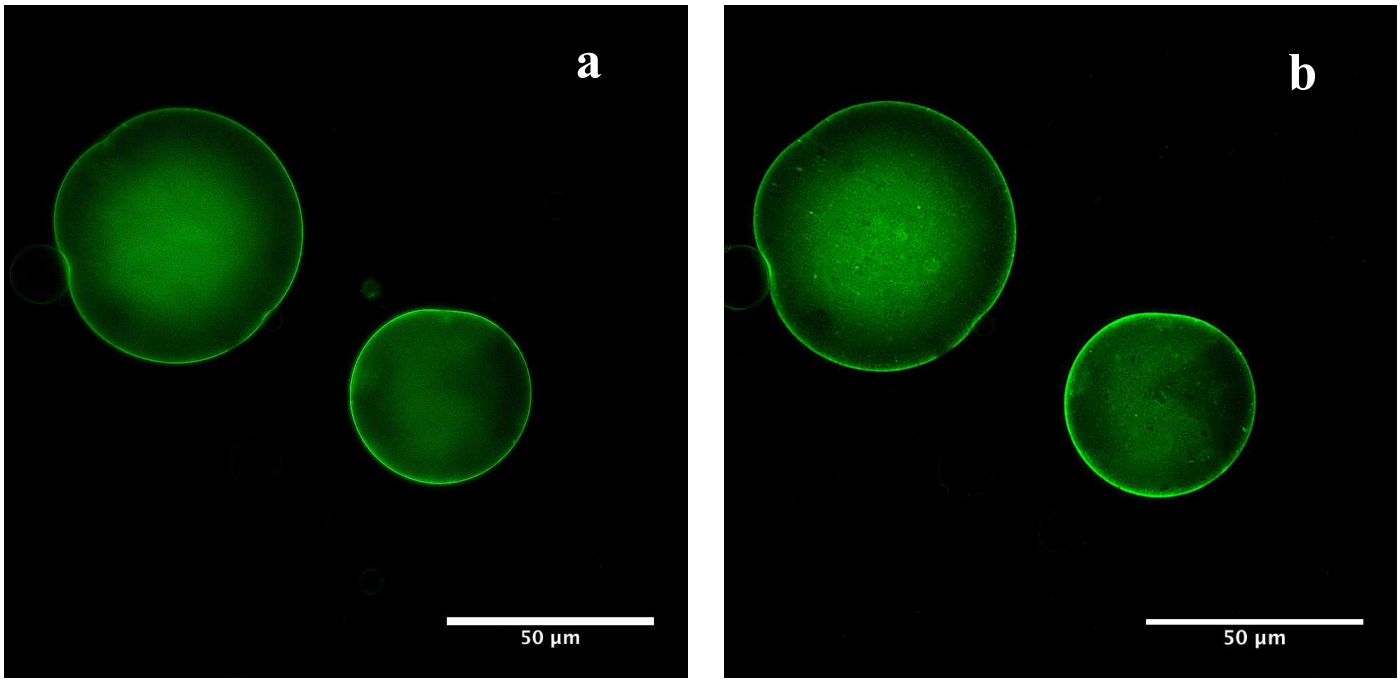

Supplementary Material

Click here to download Supplementary Material: Supporting data NFC.docx